

Available online at www.sciencedirect.com

ScienceDirect

www.elsevier.com/locate/jes

Response of soil microbial activities and ammonia oxidation potential to environmental factors in a typical antimony mining area

Aihua Wang¹, Shujun Liu², Jun Xie², Wei Ouyang^{1,3}, Mengchang He^{1,*},
Chunye Lin¹, Xitao Liu¹

¹ State Key Laboratory of Water Environment Simulation, School of Environment, Beijing Normal University, Beijing 10875, China

² Lengshuijiang Branch of Loudi Ecology and Environment Bureau, Lengshuijiang 417099, China

³ Advanced Interdisciplinary Institute of Environment and Ecology, Beijing Normal University, Zhuhai 519087, China

ARTICLE INFO

Article history:

Received 17 March 2022

Revised 1 July 2022

Accepted 4 July 2022

Available online 14 July 2022

Keywords:

Antimony mining area

Metal(loid) pollution

Microbial characteristics

Enzyme activities

Ammonia oxidation potential

ABSTRACT

Mining, smelting and tailing deposition activities can cause metal(loid) contamination in surrounding soils, threatening ecosystems and human health. Microbial indicators are sensitive to environmental factors and have a crucial role in soil ecological risk assessment. Xikuangshan, the largest active antimony (Sb) mine in the world, was taken as the research area. The soil properties, metal(loid) contents and microbial characteristics were investigated and their internal response relationships were explored by multivariate statistical analysis. The assessment of the single pollution index and Nemerow synthetic pollution index (P_N) showed that the soils were mainly polluted by Sb, followed by Cd and As, in which sampling site S1 had a slight metal(loid) pollution and the other sampling sites suffered from severe synthetic metal(loid) pollution. The microbial characteristics were dissimilar among sampling points at different locations from the mining area according to hierarchical cluster analysis. The correlation analysis indicated that fluorescein diacetate hydrolase, acid phosphatase, soil basal respiration and microbial biomass carbon were negatively correlated with P_N , indicating their sensitivity to combined metal(loid) contamination; that dehydrogenase was positively correlated with pH; and that urease, potential ammonia oxidation and abundance of ammonia-oxidizing bacteria and archaea were correlated with N (nitrogen) contents. However, β -glucosidase activity had no significant correlations with physicochemical properties and metal(loid) contents. Principal components analysis suggested bioavailable Sb and pH were the dominant factors of soil environment in Xikuangshan Sb mining area. Our results can provide a theoretical basis for ecological risk assessment of contaminated soil.

© 2022 The Research Center for Eco-Environmental Sciences, Chinese Academy of Sciences. Published by Elsevier B.V.

Introduction

Antimony (Sb) is the ninth most mined metal. According to the latest report of U.S. Geological Survey (USGS, 2022), China was the leading global Sb producer in 2021 and accounted for

* Corresponding author.

E-mail: hemc@bnu.edu.cn (M. He).

55% of global Sb mine production, followed by Russia, 23%, and Tajikistan, 12%. China also possessed the largest reserves of Sb in the world, with nearly 480,000 metric tons (USGS, 2022). Antimony and its associated compounds have been widely employed as flame retardant additives in plastics, as catalysts in the production of polyethylene terephthalate (PET) polymers, as hardeners in lead alloys, and as therapeutic agents against tropical protozoan diseases (Bagherifarn et al., 2019; Filella et al., 2002). The extensive application of Sb-containing products has intensified the mining and smelting activities of Sb ore, which caused the change of soil properties (e.g., pH and organic matter) and the accumulation of metal(loid)s (e.g., Sb, As, Pb, Cu, Zn, and Cd) in the soil environment (Li et al., 2021b; Liu et al., 2020), threatening soil ecosystem function and human health (Bolan et al., 2022; Cappuyns et al., 2021; Nguyen et al., 2021). Therefore, selecting the suitable indicators to assess the soil ecological risk in Sb mining area is very necessary (Tang et al., 2019).

Microorganisms are essential biological components of soil ecosystems that have determinant roles in maintaining soil biogeochemical cycles and ecological functioning (Bahram et al., 2018). Soil microbiological indicators, including enzyme activities, basal respiration and microbial biomass, are highly sensitive to environmental alterations, and have been broadly utilized to monitor soil contamination (Aponte et al., 2020a; Feyzi et al., 2020; Gruen et al., 2018; Tang et al., 2019). Gong et al. (2021) reported that soil urease and phosphatase activities were significantly inhibited by heavy metal pollution. The activities of dehydrogenase, arylsulfatase and β -glucosidase decreased with the metal(loid) contamination in a Cu smelter zones (Aponte et al., 2021). Niemeyer et al. (2012) pointed out that soil respiration and microbial biomass of C and N were negatively correlated with metal contamination at a Pb smelter area, indicating the high ecological risks to soil functions mediated by microbes owing to deposition of tailings contaminated with metals. Moreover, microbial activities were also regulated by the physicochemical properties of the soils. For example, the content of soil nutrients (C, N, and P) influenced the enzyme activities in nonferrous metal(loid) mining areas (Li et al., 2022; Liu et al., 2019). Higher soil clay content could weaken the negative influences of heavy metal contamination on microbial activities (Aponte et al., 2020b).

Nitrification plays an important role in biogeochemical N (nitrogen) cycle in soil. Ammonia oxidation, the first and rate-limiting step in nitrification, has been regarded as a sensitive microbial process to evaluate metal contamination, which is biologically driven by ammonia-oxidizing archaea (AOA) and ammonia-oxidizing bacteria (AOB) with functional ammonia-monooxygenase encoded by the *amoA* gene (Li et al., 2019; Tang et al., 2019). Previous studies have reported that metal(loid)s of (e.g., Cu, As, and Hg) had a negative impact on the soil ammonia oxidation rate and abundance of ammonia-oxidizing microorganisms (He et al., 2018; Subrahmanyam et al., 2014; Zhou et al., 2015). Liu et al. (2018) stated that soil nitrification rate and abundance of ammonia oxidizers were affected by compound heavy metal pollution of soils in the vicinity of a tailings dam, which might be considered as useful biological indicators to assess metal stress on soil ecosystems. Moreover, soil physico-

chemical properties, such as pH, clay content and NO_3^- -N, also shaped the AOA and AOB abundance (Li et al., 2021a; Wang et al., 2023).

The Xikuangshan Sb mine, which is located in Lengshuijiang City in Hunan Province of China, has the largest Sb deposition in the world and is known as the “World Capital of Antimony”. Previous studies have demonstrated that the soils around the Xikuangshan Sb deposit were seriously polluted by metal(loid)s, especially Sb and As (Guo et al., 2014; Okkenhaug et al., 2011; Zhang et al., 2018). The community composition of bacteria, fungi and archaea in soil in this Sb mining area was shaped by the Sb content, pH and soil texture (Wang et al., 2019, 2022). However, there are limited studies on the response of microbial activities and ammonia oxidation to environmental factors and the screening of sensitive microbial indices to diagnose the status of soil pollution in Sb deposit. Hence, the objectives of our study were (1) to assess the metal(loid) pollution in the Sb mine-affected soils, (2) to explore the characteristics of enzyme activities, basal respiration, microbial biomass and ammonia oxidation potential in different sampled polluted sites, (3) to derive the relationships of microbial indicators with soil properties and metal(loid) pollution in the Xikuangshan Sb mining deposit. The results can provide sensitive microbial indicators for ecological risk assessment of contaminated soil and contribute to decision-making risk management to protect soil ecosystem.

1. Materials and methods

1.1. Soil samples collection

Eight representative sampling sites of agricultural soils around Xikuangshan Sb mining area were selected. At each sampling site, three soil samples were randomly collected and thoroughly mixed. Sampling points marked with S plus numbers are shown in Fig. 1. The S1 sampling site was located between the mining area and the river. Soil samples S2, S3, S4, and S5 were collected within the proximity of the Sb smelter. S6, S7 and S8 were located around the mine, downstream of the Lianxi River and Qingfeng River. At each site, 0–20 cm surface soils were collected and placed into sterile plastic bags after removing the roots, plant residues and stones. A portion of each soil sample was stored in a refrigerator at 4°C for microbial indicator analysis, and the remaining portion was air-dried and passed through a 10-mesh (< 2 mm) sieve for subsequent analysis of physicochemical property and metal(loid) content.

1.2. Soil physicochemical properties and metal(loid) content analysis

Soil pH was measured in a mixture of soil with 0.01 mol/L CaCl_2 (AR: 99.0%, Sinopharm Chemical Reagent, China) solution (1:5, m/V) using a pH meter (PB-10, Sartorius, Germany) according to the method of Soil quality - Determination of pH (ISO 10390:2005). Total organic carbon (TOC) and total nitrogen (TN) were measured by an elemental analyzer (EA3000, EuroVector, Italy). Before measuring the TOC, the soil samples were acidified with 1 mol/L HCl to remove inorganic carbon.

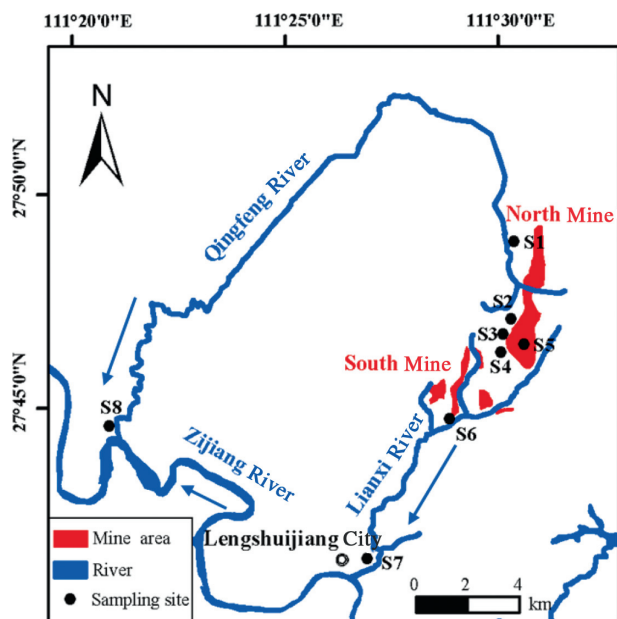


Fig. 1 – Location of soil sampling sites (S1–S8) in the study area.

A laser particle size analyzer (S3500, Microtrac, USA) was utilized to determine the soil texture. The $\text{NH}_4^+\text{-N}$ and $\text{NO}_3^-\text{-N}$ in the soil samples were extracted by 2 mol/L KCl (AR: 99.5%, Sinopharm Chemical Reagent, China) with a soil:solution ratio of 1:5 (m/V) and measured by a flow analyzer (AACE, SEAL, Germany).

Soil samples sifted with a 100-mesh sieve were digested with 3:1:1 (V/V/V) $\text{HCl:HNO}_3:\text{HClO}_4$ (GR: 99.8%, Tianjin Fuchen Chemical Reagent Factory, China) in triplicate using a microwave digestion instrument to determine the total metal(loid) contents. A standard soil reference material (GBW07407) and blank sample were digested and determined in triplicate in the same procedures performed on samples for quality assurance and control (Zhang et al., 2018). Total Sb and As contents were measured by hydride generation atomic fluorescence spectrometry (HG-AFS) (AFS-9700, Haiguang Instrument, China). The total contents of Cd, Zn, Cu, Cr, Fe, and Mn were measured by inductively coupled plasma atomic emission spectrometry (ICP-AES) (NexION 300x, PerkinElmer, USA). Bioavailable Sb was specifically determined due to its highest content. Deionised water and 0.01 mol/L CaCl_2 were employed to extract bioavailable Sb in triplicate with a solid:solution ratio of 1:10 (W/V) by shaking for 2 hr at 20°C (Ettler et al., 2007).

1.3. Metal(loid) pollution indices

The single pollution index (P_i) and Nemerow synthetic pollution index (P_N) were selected to evaluate the single pollution and comprehensive pollution, respectively, of metal(loid)s based on the total metal(loid) content. P_i is helpful in assessing the most dangerous metal(loid) within the analyzed elements, and P_N is selected for calculating the comprehensive contamination degree of metal(loid) in the soil environment (Cheng et al., 2007). P_i and P_N are calculated as Eqs. (1) and (2):

$$P_i = \frac{C_i}{S_i} \quad (1)$$

$$P_N = \sqrt{\frac{P_{i(\text{ave})}^2 + P_{i(\text{max})}^2}{2}} \quad (2)$$

where, C_i (mg/kg) is the measured content of metal(loid) i ; S_i (mg/kg) is the standard reference value of metal(loid) i in the soil; $P_{i(\text{max})}$ (mg/kg) is the maximum value of the single pollution index of all metal(loid)s; $P_{i(\text{ave})}$ (mg/kg) is the average value of the single pollution index of all metal(loid)s.

In this study, the standard reference value of Sb is 78 mg/kg based on the ecological soil screening levels (Eco-SSLs) of U.S. Environmental Protection Agency (USEPA, 2005). The standard values of As, Cd, Zn, Cu and Cr refer to “Soil environmental quality-Risk control standard for soil contamination of agricultural land” (GB 15618-2018) according to soil pH. The contents of Fe and Mn are chosen as soil physiochemical properties, but their pollution as heavy metals are not considered. The results of P_N are divided into five pollution classes: $P_N \leq 0.7$, safe; $0.7 < P_N \leq 1.0$, warning line; $1.0 < P_N \leq 2.0$, slight pollution; $2.0 < P_N \leq 3.0$, moderate pollution; and $P_N > 3.0$, heavy pollution (Cheng et al., 2007).

1.4. Soil enzyme activities

Five enzyme activities, namely, fluorescein diacetate (FDA) hydrolase, dehydrogenase, urease, acid phosphatase and β -glucosidase, were measured according to the methods reported by Wang et al. (2021). FDA hydrolase activity was quantified by the amount of fluorescein hydrolyzed from FDA using a UV spectrophotometer (Adam and Duncan, 2001). Dehydrogenase activity was determined by the value of triphenyl formazan (TPF) produced by the reduction of 2,3,5-triphenyl tetrazolium chloride (TTC) (Dick, 2011). Using urea as the substrate, urease activity was measured by the release of ammonium after incubation. Acid phosphatase and β -glucosidase activities were determined by the release of p -nitrophenol (PNP) from the substrate of p -nitrophenyl-phosphate and p -nitrophenyl- β -D-glucopyranoside, respectively (Dick, 2011). The enzyme assays were measured with fresh soils in triplicate, and the reactions without added substrate were designed as blank controls. Biochemical reagents used for enzyme activity determination were purchased from Sigma-Aldrich (USA) with a purity $\geq 99.0\%$.

1.5. Soil basal respiration, microbial biomass carbon and metabolic quotient

Soil basal respiration (SBR) and microbial biomass carbon (MBC) were measured in triplicate based on the experimental procedure of Wang et al. (2021). SBR was estimated by measuring the amount of CO_2 with a gas chromatograph (7890B, Agilent Technologies, USA) evolved from the incubated soil in a closed system. MBC was measured by the chloroform fumigation-extraction method (Vance et al., 1987). The soil microbial metabolic quotient ($q\text{CO}_2$) was calculated from the ratio of SBR to MBC and expressed as $\mu\text{g CO}_2/(\text{mg C}_{\text{MBC}} \cdot \text{hr})$ (Anderson and Domsch, 1993).

1.6. Potential ammonia oxidation rate

The potential ammonia oxidation (PAO) rate was measured by a chlorate inhibition method in triplicate and expressed by the amount of NO_2^- -N. Briefly, fresh soil (dry weight 5.0 g) was added to 50-mL centrifuge tubes containing 20 mL phosphate buffer solution (PBS) (g/L: NaCl 8.0, KCl 0.2, Na_2HPO_4 0.2, and NaH_2PO_4 0.2; pH 7.4) with 1 mmol/L $(\text{NH}_4)_2\text{SO}_4$, and then 10 mM potassium chlorate was added to inhibit NO_2^- -N oxidation. The suspension was incubated in a dark incubator at 25°C for 24 hr, and then NO_2^- -N was extracted with 5 mL of 2 mol/L KCl and determined by a spectrophotometer at a wavelength of 540 nm with N-(1-naphthyl) ethylenediamine dihydrochloride (Wang et al., 2021).

1.7. Soil DNA extraction and quantitative PCR assay

DNA was extracted from 0.5 g soil using the E.Z.N.A.TM Mag-Bind Soil DNA Kit (OMEGA, USA) according to the manufacturer's protocol instructions. The concentration and purity of DNA were determined by Nanodrop Technologies to ensure DNA purity (OD260/OD280) within the range of 1.8 to 2.0. The abundance of AOB and AOA involved in the conversion of NH_4^+ -N to NO_2^- -N was quantified by the amount of the *amoA* gene. The *amoA* gene of AOB was amplified with the primers *amoA*-1F (5'-GGG GTT TCT ACT GGT GGT-3') and *amoA*-2R (5'-CCC CTC KGS AAA GCC TTC TTC-3'), and the *amoA* gene of AOA was amplified with the primers Arch-*amoA*F (5'-STA ATG GTC TGG CTT AGA CG-3') and Arch-*amoA*R (5'-GCG GCC ATC CAT CTG TAT GT-3') (Zhou et al., 2015). The copy numbers of the AOB-*amoA* and AOA-*amoA* genes were measured by quantitative PCR (qPCR) with the 7500 Fast Real-time PCR System (Applied Biosystems, USA).

The 25 μL qPCR mixture contained 12.5 μL SYBR Premix Ex Taq II (2 \times) (TaKaRa Biotechnology, China), 1 μL of each primer (10 $\mu\text{mol/L}$), 0.5 μL ROX Reference Dye II (50 \times), 2 μL template DNA and 8 μL ddH₂O. The qPCR protocols were performed as follows: 50°C, for 2 min and 95°C for 10 min, followed by 45 cycles of 30 sec at 95°C, 40 sec at 58°C (for AOB) and 56°C (for AOA), and 1 min at 72°C. Serial dilutions of a known copy number of plasmid DNA were applied to perform qPCR assays to generate standard curves. The linear coefficient correlation (R^2) of the standard curves exceeded 0.99. The *amoA* gene abundance of AOB and AOA was calculated based on the constructed standard curves.

1.8. Statistical analysis

The statistical analyses of experimental data were performed by Microsoft Excel and SPSS 25.0. The sampling site was constructed in ArcGIS 10.2 and graphs were drawn by Origin 2021. Normality and homoscedasticity assumptions were evaluated by Shapiro-Wilks and Levene tests, respectively. For normal and homogeneous experimental variables, one-way analysis of variance (ANOVA) followed by Duncan's multiple range test was performed to analyze the differences in the mean values among the different samples. Kruskal-Wallis test was used for multiple comparison for variables that did not meet the assumptions. Different letters were used to represent significant ($p < 0.05$) discrepancies. The heatmap of the correlation

analysis was constructed based on Spearman's correlation coefficient using Origin 2021. Hierarchical cluster analysis was performed to classify soils based on microbial properties using SPSS 25.0. Principal components analysis (PCA) was performed to exhibit the relationship between physicochemical properties and microbiological parameters, which was carried out with the packages "FactoMineR" and "factoextra" of R version 4.1.1.

2. Results

2.1. Soil physicochemical properties and metal(loid) contents

The basic physicochemical properties of the soils in the sampling area are presented in Table 1. The soil pH values fell in the range of 4.8–7.7. The soils of S2, S3 and S5 were acidic (pH < 6.5), while the soils of S4, S6 and S8 were alkaline (pH > 7.5). The TOC content of the soil samples ranged from 0.7% to 3.8%, with the lowest TOC at sampling site S4 and the highest TOC at S5. The ranges of NH_4^+ -N and NO_3^- -N were 3.0–15.0 mg/kg and 3.0–13.5 mg/kg, respectively. Soil samples were classified as loam or clay loam according to the international standard for soil texture classification. The contents of total Fe and total Mn varied from 25.1 to 41.8 g/kg and from 0.22 to 0.63 g/kg, respectively.

The total contents of Sb, Cd, As, Zn, Cu and Cr ranged from 106 to 4613 mg/kg, from 0.6 to 6.5 mg/kg, from 25 to 246 mg/kg, from 65 to 324 mg/kg, from 17.5 to 58.7 mg/kg, and from 51.9 to 91.4 mg/kg, respectively. In general, there were significant ($p < 0.05$) differences in metal(loid) contents among the sampling sites (Table 1). P_i was used to evaluate the contamination degree of a single metal(loid) in the soils. The total Sb contents at all the sampling sites exceeded the standard value of Eco-SSLs for Sb (78 mg/kg) in U.S. Environmental Protection Agency (USEPA, 2005). Total contents of Cd and As exceeded the soil environmental quality risk control standard values for soil contamination of agricultural land in China (GB 15618-2018), except for sampling site S1. For Zn, the contents of sampling sites S6 and S7 surpassed the standard values. The Cu and Cr contents at all sampling sites did not exceed the environment quality criteria. The rank of metal(loid) pollution in the study area was Sb > Cd \approx As > Zn \approx Cu \approx Cr based on P_i . Antimony was the most polluted element, followed by Cd and As (Fig. 2a). P_N could reflect the comprehensive pollution degree of metal(loid)s at each sampling site, and there were spatial differences in the metal(loid) pollution in the soil of each sampling point. P_N at S1 had the lowest value of 1.47, which was classified as a slight pollution level. However, P_N at the other sampling sites was greater than 3.0, which was classified as a heavy pollution level, in which sampling site S2 had the most serious metal(loid) pollution (Fig. 2b).

According to metal(loid) contamination levels, the available contents of Sb, which was the most heavily contaminated metal, were determined. The bioavailable Sb contents extracted from H₂O and 0.01 mol/L CaCl₂ in S1–S8 were in the ranges of 0.5–27.0 mg/kg and 0.3–21.7 mg/kg (Table 1), respectively, which only accounted for a small proportion of the total Sb. The proportion extracted with H₂O ranged from 0.30%

Table 1 – Basic physiochemical properties and metal(loid) contents of the soil samples.

| Sample site | pH | TOC (%) | NH ₄ ⁺ -N (mg/kg) | NO ₃ ⁻ -N (mg/kg) | Clay (%) | Silt (%) | Sand (%) | Fe (g/kg) | Mn (g/kg) | Sb (mg/kg) | Cd | As | Zn | Cu | Cr | SbH ₂ O | SbCaCl ₂ |
|-------------|-----|---------|---|---|----------|----------|----------|-----------|-----------|------------|----------|--------|---------|-----------|-----------|--------------------|---------------------|
| S1 | 6.8 | 2.4 | 3.0 | 12.8 | 18.5 | 48.5 | 33.0 | 32.7 | 0.39 | 112±7g | 0.6±0.0g | 26±1f | 70±4g | 17.8±0.2g | 59.4±0.6g | 0.6±0.1f | 0.3±0.0h |
| S2 | 5.4 | 0.9 | 15.0 | 3.0 | 12.6 | 42.6 | 44.8 | 29.9 | 0.22 | 4560±77a | 2.0±0.1c | 180±8b | 120±8de | 26.3±0.6e | 63.5±0.7f | 26.9±0.5a | 21.5±0.3a |
| S3 | 5.0 | 1.5 | 12.8 | 7.6 | 17.4 | 47.4 | 35.2 | 40.7 | 0.40 | 432±5e | 1.6±0.0e | 75±6c | 113±2e | 32.8±0.4d | 86.6±0.8b | 1.3±0.1f | 0.6±0.0b |
| S4 | 7.7 | 0.7 | 5.3 | 9.6 | 21.6 | 51.6 | 26.8 | 25.1 | 0.24 | 1361±31b | 0.8±0.0f | 236±8a | 88±1f | 20.5±1.0f | 52.3±0.4h | 24.9±1.2b | 19.8±0.3b |
| S5 | 4.8 | 3.8 | 6.2 | 12.7 | 12.0 | 42.0 | 46.0 | 32.6 | 0.46 | 828±5d | 1.8±0.0d | 82±3c | 143±2c | 47.1±1.6b | 79.3±0.6d | 6.8±0.1c | 3.5±0.1c |
| S6 | 7.6 | 1.7 | 6.7 | 10.8 | 13.6 | 43.6 | 42.8 | 37.7 | 0.52 | 316±1f | 6.4±0.1a | 50±4e | 313±9a | 39.5±0.4c | 77.2±0.8e | 2.7±0.0e | 1.7±0.0f |
| S7 | 7.4 | 2.9 | 3.1 | 13.3 | 16.0 | 46.0 | 38.0 | 41.8 | 0.47 | 328±8f | 3.5±0.1b | 53±4de | 288±4b | 55.7±2.4a | 81.3±0.6c | 4.0±0.1d | 2.6±0.1e |
| S8 | 7.6 | 2.6 | 3.0 | 13.5 | 18.7 | 48.7 | 32.6 | 31.2 | 0.63 | 1228±12c | 1.7±0.1e | 63±2d | 109±3e | 34.9±0.5d | 90.4±0.9a | 4.2±0.1d | 2.9±0.2d |

Note: Fe and Mn are selected as soil physiochemical properties, and their pollution is not considered heavy metals. Clay, silt, and sand represent soils with particle sizes of 0-2, 2-20, and 20-2000 µm, respectively. Different letters indicate significant differences among the different sites (*p* < 0.05). TOC: total organic carbon.

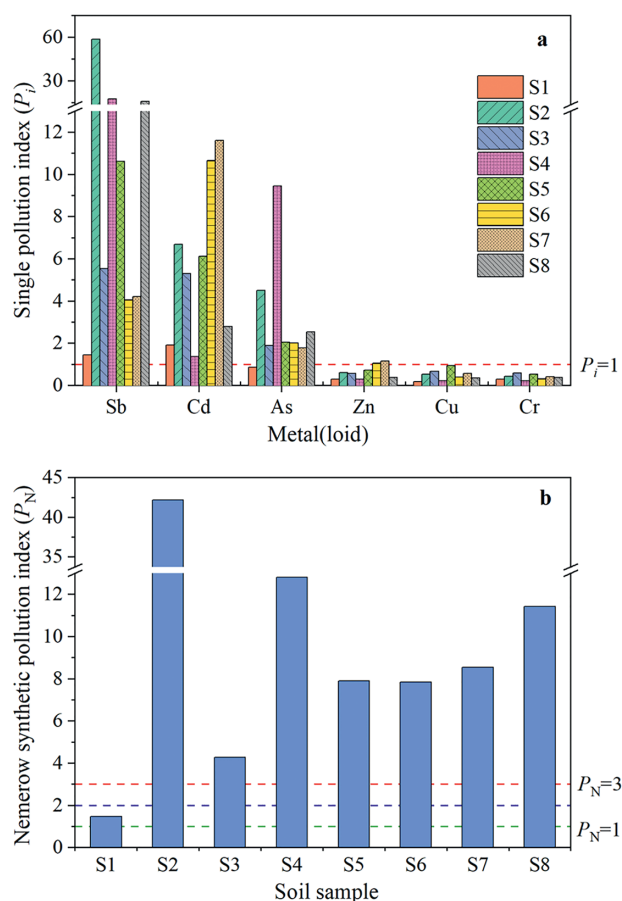


Fig. 2 – (a) Single pollution index (P_i) and (b) Nemerow synthetic pollution index (P_N) of the soil samples.

to 1.83%, and the proportion extracted with 0.01 mol/L CaCl₂ ranged from 0.14% to 1.75%.

2.2. Soil enzyme activities

The five enzyme activities of FDA hydrolase, dehydrogenase, urease, acid phosphatase and β -glucosidase are illustrated in Fig. 3. FDA hydrolase activity ranged from 9.7 to 69.5 μg fluorescein/(g soil·hr). The lowest activity was determined in the soil from the extremely polluted site of S2 (Fig. 3a). The dehydrogenase activity values were in the range of 0.17–2.38 μg TPF/(g soil·hr), among which higher dehydrogenase activities appeared at S6, S7 and S8 far from the mining area, and lower dehydrogenase activities appeared at S2, S3, S4 and S5 near the mining area (Fig. 3b). The activities of urease and acid phosphatase significantly ($p < 0.05$) differed among the sampling sites. The lowest urease activity (3.1 μg NH₄⁺-N/(g soil·hr)) and lowest acid phosphatase activity (53.5 μg PNP/(g soil·hr)) were observed in S2, which was heavily polluted, while the highest urease activity (32.3 μg NH₄⁺-N/(g soil·hr)) and highest acid phosphatase activity (452.9 μg PNP/(g soil·hr)) occurred in S8 and S3, respectively (Fig. 3c and d). The values of β -glucosidase activity were in the range of 13.1–45.5 μg PNP/(g soil·hr). The S1 sampling site with slight pollution had

the highest β -glucosidase activity, yet the S4 sampling site had the lowest β -glucosidase activity (Fig. 3e).

2.3. Soil basal respiration, microbial biomass carbon and metabolic quotient

The intensities of SBR, MBC and qCO₂ in the mining area are shown in Fig. 4. SBR and MBC ranged from 12.0 to 41.5 μg CO₂/(g soil·day) and from 74.6 to 148.8 μg /g soil, respectively. SBR and MBC were relatively higher at sampling sites S1 and S3 with a lower pollution index but relatively lower at sampling sites S2 and S4 with a higher pollution index (Fig. 4a and b), which demonstrated that long-term metal(loid) contamination had a negative effect on soil microorganisms. The range of qCO₂ was 4.4–16.0 μg CO₂/(mg C_{MBC}·hr). There were significant ($p < 0.05$) differences among sampling sites S1, S2, and S6 based on the results of one-way ANOVA, in which the maximum qCO₂ appeared at sampling point S1 and the lower qCO₂ appeared at sampling points S2 and S6 (Fig. 4c).

2.4. Potential ammonia oxidation rate and abundance of AOA and AOB

The PAO ranged from 0.24–7.13 μg NO₂⁻-N/(g soil·day), in which the values at S6, S7 and S8 far from the mining area were relatively higher, while the values at S2, S3, S4 and S5 close to the mining area were relatively lower (Fig. 5a). The results showed that the mining activity could affect ammonia oxidation in soils. AOA and AOB communities participate in the ammonia oxidation and both contain the *amoA* gene that encodes ammonia monooxygenase. AOB-*amoA* gene abundance in the soil samples ranged from 9.27×10^3 to 4.38×10^8 copies/g soil, and AOA-*amoA* gene abundance ranged from 1.82×10^5 to 3.34×10^9 copies/g soil. The copy number of the AOA-*amoA* gene was higher than that of the AOB-*amoA* gene at each sampling site. The changes in AOA and in AOB among the sampling sites were similar, with higher abundances in S7 and S8 far from the mining area and lower abundances in S2, S3, S4 and S5 near the mining area (Fig. 5b).

2.5. Multivariate statistical analysis

The correlations among soil physicochemical properties, metal(loid) contents and microbial parameters in the mining soil based on Spearman's correlation coefficients are shown in Fig. 6 and Appendix A Figs. S1–S2. There were significantly ($p < 0.01$) positive correlations among total Sb and bioavailable Sb extracted with H₂O and CaCl₂ (Appendix A Fig. S1), demonstrating the internal effect of total Sb on bioavailability. Total Sb and two kinds of bioavailable Sb had significantly ($p < 0.05$) positive correlations with total As and P_N (Appendix A Fig. S1), which indicated that Sb and As might coexist in soil environment and dominated the pollution situation in the mining area. FDA enzyme activity showed significantly ($p < 0.05$) negative correlations with the two kinds of available Sb and P_N. Acid phosphatase activity also showed a significantly ($p < 0.05$) negative correlation with P_N, manifesting the influence of metal(loid) comprehensive pollution. The activities of dehydrogenase and urease were positively ($p < 0.05$) correlated with soil pH and NO₃⁻-N, respectively. However, β -glucosidase

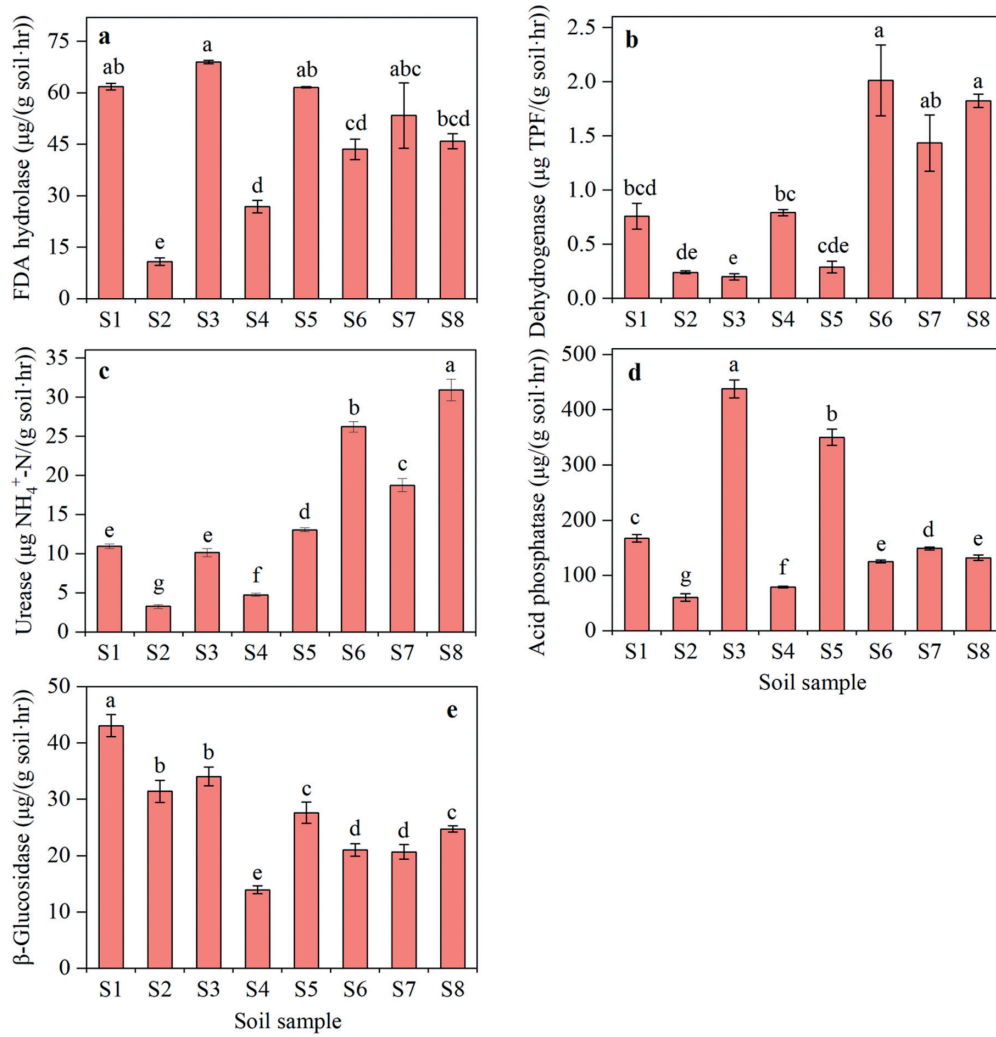


Fig. 3 – Enzyme activities in the soil samples. (a) Fluorescein diacetate (FDA) hydrolase activity; (b) Dehydrogenase activity; (c) Urease activity; (d) Acid phosphatase activity; (e) β-Glucosidase activity. Data are shown as average ± standard deviation. Different letters above the bars indicate significant differences among the different sites ($p < 0.05$).

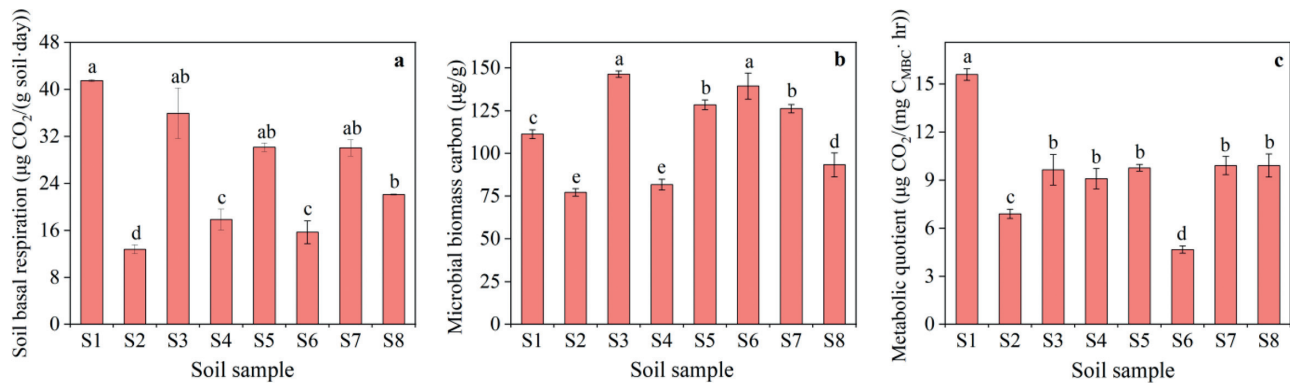


Fig. 4 – (a) Soil basal respiration (SBR), (b) Microbial biomass carbon (MBC), and (c) Metabolic quotient (qCO₂) of soil samples from each site. Data are shown as average ± standard deviation. Different letters above the bars indicate significant differences among the different sites ($p < 0.05$).

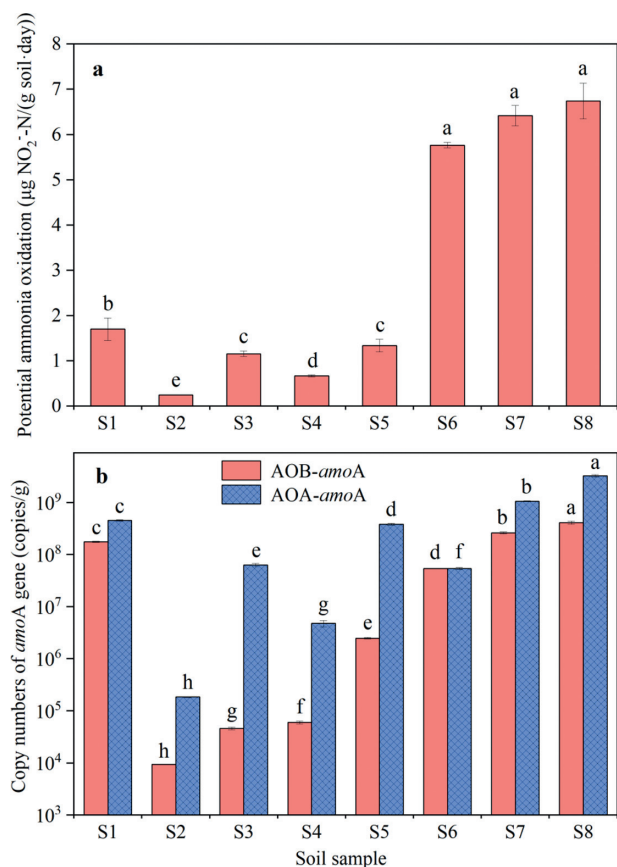


Fig. 5 – (a) Potential ammonia oxidation (PAO) and (b) copy numbers of AOB-amoA and AOA-amoA genes in the soil samples. Data are shown as average \pm standard deviation. Different letters above the bars indicate significant differences among the different sites ($p < 0.05$).

activity had no significant correlations with physicochemical properties and metal(loid) contents. Significantly ($p < 0.05$) negative relationships between MBC, SBR with P_N were observed. The PAO and abundance of AOB and AOA had significantly ($p < 0.05$) negative correlations with NH_4^+ -N and significantly ($p < 0.05$) positive correlations with NO_3^- -N, indicating the effect of the N content. In addition, the PAO rate was also negatively ($p < 0.05$) associated with total As (Fig. 6).

The correlations among the microbial indicators showed that FDA enzymes, acid phosphatase activity and SBR had significantly ($p < 0.01$) positive connections. A statistically significant ($p < 0.05$) positive relationship between SBR and qCO_2 was also observed. Moreover, the microbial parameters of urease activity, PAO, and abundance of AOB and AOA related to nitrogen cycle processes had significant positive relationships, demonstrating their intrinsic connections in soil N transformation (Appendix A Fig. S2). Hierarchical clustering analysis based on the 11 microbial indicator data of each sampling site showed that S1, S2, S3, S4 and S5 near the Sb mining area were clustered together, while S6, S7 and S8 far from the mining area were clustered together, indicating that mining activities affected the soil microbial characteristics (Fig. 7).

To further explain the relationships between environmental factors, metal(loid) contents and microbial indicators, PCA was performed (Appendix A Fig. S3). The first dimension could explain 39.7% of variations, in which two kinds of extractable Sb occupied the primary negative loadings. In addition, total Sb, total As and P_N also occupied certain negative loadings on the first coordinate. The second dimension could explain 20.7% of variations, which dominated by pH and soil texture. It could be observed that dehydrogenase, abundance of AOA and AOB, PAO, and urease showed similar contributions in the coordinate system based on the results of PCA.

3. Discussion

3.1. Pollution analysis of soil metal(loid)

In this study, the soils at almost all the sampling sites were contaminated with Sb, As and Cd, of which Sb was the most serious metal(loid) pollutant, which is consistent with the finding of Wei et al. (2015) that the Xikuangshan mine experienced severe Sb pollution and showed high ecological risk. Moreover, other Sb mining areas, such as the largest Hg–Sb mine in Qinling Orogen of China, San Antonio Sb mine in Spain and Mau Due Sb mine in North Vietnam, also exhibited high contamination level of Sb in soils (Cappuyns et al., 2021; Murciego Murciego et al., 2007; Qin et al., 2022). Furthermore, the results of P_N showed that the sampling sites suffered from heavy comprehensive metal(loid) pollution except for S1, which might be associated with mining, smelting, and fly ash sinks and solid waste deposits, and resulted in the continuous release of metal(loid) into the environment (Cappuyns et al., 2021; Guo et al., 2014).

The total contents of metal(loid)s usually can reflect the pollution status of soil, but may not represent a bioavailable fraction. Wang et al. (2007) pointed out that the potential effects of heavy metal on microbial activity depend on its available form in the soil. Single-step extraction methods with deionized water and $CaCl_2$ are commonly employed to assess the bioavailability of Sb in soil (Ettler et al., 2007; Zhang et al., 2018). The extracted fraction of Sb was only accounted for a small proportion of total content, which reaches a consensus to results of Ettler et al. (2007). Extractable Sb had weak binding capacity with mineral lattice, Fe and Mn oxides and organic matter, showing the high mobility and biological toxicity risk in soil (He et al., 2019; Li et al., 2021b). According to the correlation analysis, the extracted amount of Sb was strongly dependent on the total Sb content and had a positive correlation with total As. These results are consistent with the result of Ettler et al. (2007) that the extractable Sb was significantly correlated with total Sb and As, which further confirms the previous observations that Sb and As often co-occur in soils around Sb mining sites (Li et al., 2021b; Sun et al., 2017).

3.2. Characteristics of microbial indicators

Soil enzymes are mainly produced by microbes and are crucial participants in soil biogeochemical processes; their activities have served as potential biological indicators to reflect the ecological effects of heavy metal in soil

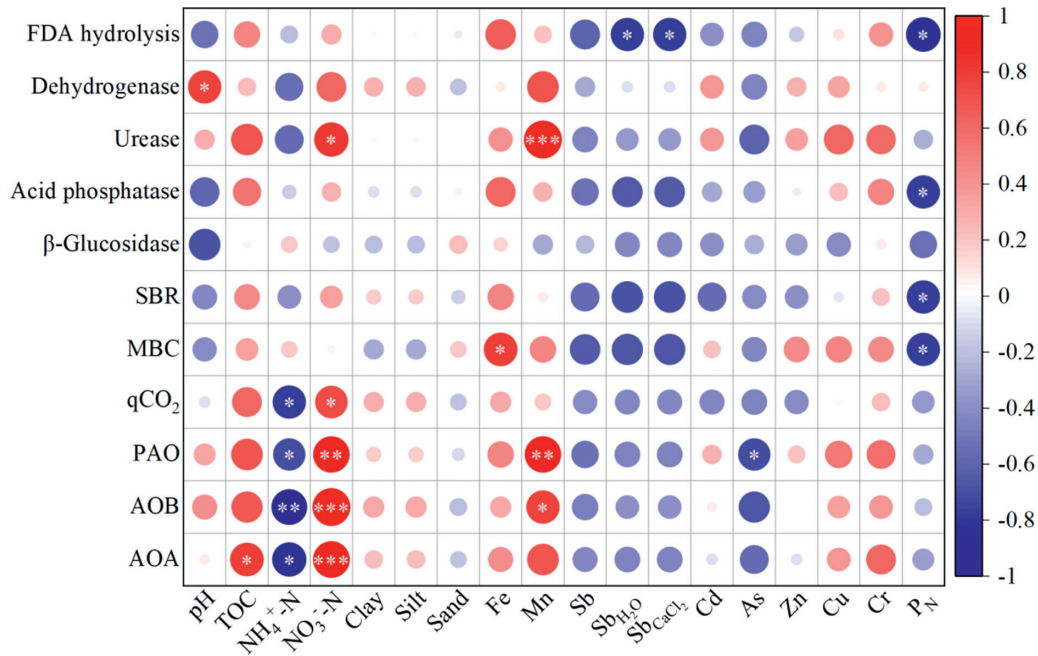


Fig. 6 – Heatmap of correlations between environmental factors and microbial indicators in the mining soil based on Spearman’s correlation coefficients. Red and blue colors represent the positive correlation and negative correlation, respectively. Asterisks indicate statistical significance at 2-tailed (* $p < 0.05$, ** $p < 0.01$, * $p < 0.001$). SbH₂O: extractable Sb with H₂O; SbCaCl₂: extractable Sb with CaCl₂; P_N: Nemerow synthetic pollution index; FDA: fluorescein diacetate; SBR: soil basal respiration; MBC: microbial biomass carbon; qCO₂: metabolic quotient; PAO: potential ammonia oxidation; AOB: ammonia oxidizing bacteria; AOA: ammonia oxidizing archaea.**

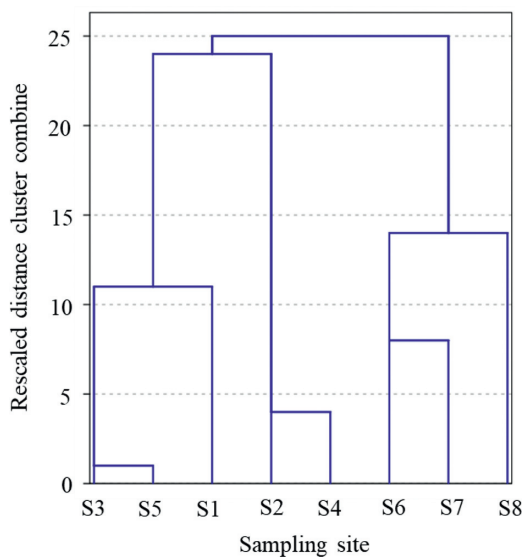


Fig. 7 – Hierarchical clustering of sampling sites based on microbial indicator data.

(Aponte et al., 2020b). Soil enzymes are mainly produced by microbes and are crucial participants in soil biogeochemical processes; their activities have served as potential biological indicators to reflect the ecological effects of heavy metal in soil (Aponte et al., 2020b). FDA hydrolysis dehydrogenase represent total soil microbial activity and functional activity,

respectively. Urease, acid phosphatase and β -glucosidase are participated in the N, P, and C cycles in soil, and their activities indicate the soil biogeochemical cycle potential. In general, our study provides evidence that enzyme activity differed among the sampling sites. The lowest activities of FDA hydrolyase, urease and acid phosphatase occurred at S2 with the most serious metal(loid) pollution, which is consistent with the result of Tang et al. (2022) that mining soils with the higher pollution degree of heavy metals exhibited the lower the soil enzyme activities. Possible explanations for the inhibition of enzyme activity are that heavy metals could interact with the sulfhydryl groups or protein active groups and denature the enzyme protein, thus inactivating enzyme activity (Das et al., 2013). However, β -glucosidase associated with soil C cycle presented higher activity in metal(loid) contaminated sites, which is different from the result of Aponte et al. (2020b) that β -glucosidase activity was inhibited by the overall level of heavy metal contamination. These results further clarify that the response of different enzymes to soil pollution is very complex (Liu et al., 2020).

Soil microbiological parameters of SBR and MBC have been recommended as potential indicators to represent the soil activity and function of heavy metal contaminated soils (Feyzi et al., 2020). The values of SBR and MBC in the heavily polluted sampling sites were significantly lower than those in the relatively less polluted sampling sites in this study, indicating the negative influence of metal(loid) pollution on microbial activity in mining soils. This finding is consistent with the research of Tang et al. (2022) that serious heavy

metal pollution in the soil near the tailings pond could cause the reduction of SBR. Gong et al. (2021) also stated that the value of MBC in soil contaminated with long-term heavy metals was lower than that in noncontaminated soil samples. Microbial qCO_2 is the ratio of SBR to MBC, which can reflect the microbial metabolism potential. S1 with the lowest metal(loid) pollution was characterized by the highest metabolic activities, and S2 and S6 with higher metal(loid) pollution had lower metabolic activities. Higher microbial qCO_2 under metal pressure often explains why soil microorganisms need more energy for survival to increase metabolism, whereas lower qCO_2 usually indicates that the utilization rate of substrate by soil microorganisms decreases, representing a reduction in metabolism. This result conformed the finding of Liu et al. (2019) that the tailings polluted by heavy metals had low microbial metabolism capacity. However, this result differs from the reports of other studies that soil-contaminated heavy metals caused an increase in qCO_2 (Niemeyer et al., 2012; Raiesi and Sadeghi, 2019). Additionally, other factors, such as the pH, texture and organic matter content of the soil, might also influence the qCO_2 of soil microbes (Insam et al., 1996).

The soil ammonia oxidation and ammonia-oxidizing microbes have important roles in nitrogen cycling. In this study, the PAO rate and the abundance of AOB and AOA were lower in the soil environment near the mining area, indicating that metal(loid) pollution caused by mining activities affected soil nitrogen cycling and related microbes. These results are similar to the finding of Liu et al. (2018) that the PAO rate and abundance of AOB and AOA were significantly different between heavily polluted soils and slightly polluted soils in the vicinity of a tailings dam. In addition, previous studies have observed that AOA had a wider distribution and that its abundance was greater than that of AOB (Subrahmanyam et al., 2014), which is consistent with the findings of our research. A possible reason for this phenomenon is that AOA has greater metal tolerance and adaptability than AOB under chronic environmental stress due to the particular chemical structure of archaeal membrane lipids, leading to the lower permeability of archaeal membranes to ions than bacterial membranes (He et al., 2018; Subrahmanyam et al., 2014).

Hierarchical cluster analysis is a method that can reflect the association of each sampling point, which was used to analyze the spatial heterogeneity of soils with different metal(loid) pollutions according to their microbial parameters (Zhang et al., 2010). The sampling points with close clustering distance were relatively similar, while the sampling sites with far clustering distance were relatively dissimilar. Our results suggested that the soils near the mining area had different microbiological characteristics with the soils far away from the mining area, which confirmed that the mining soils polluted by metal(loid) were highly discriminated by soil microbial parameters (Zhang et al., 2010).

3.3. Relationships of microbial indicators with soil properties and metal(loid)s

The results of correlation analysis showed that microbial indicators are affected by soil physiochemical properties and metal(loid)s. FDA hydrolase activity was negatively corre-

lated with extractable Sb and had no significant correlation with total Sb, demonstrating that bioavailable Sb was better than total Sb to reflect its effect on FDA hydrolase activity. Zhu et al. (2018) also suggested that the content of extractable Sb significantly affected the characteristics of the soil microbes. The potentially available fraction of metal elements could better explain the change in enzyme activity than that of the total fractions (Pedro Martin-Sanz et al., 2018). In addition, FDA and acid phosphatase activities had negative relationships with P_N , which indicated that the combined metal(loid) pollution also influenced the enzyme activity and potential ecological functioning (Aponte et al., 2020a). Dehydrogenase activity had no significant correlations with metal(loid) contents in soil but had a significant positive correlation with soil pH, which is consistent with the finding of Yang et al. (2016) that pH was the most significant environmental factor for soil enzyme activity. As a soil core parameter, pH could affect the dissociation state of the enzyme active sites and enzyme stability (Yang et al., 2016), which might explain the effect of pH on dehydrogenase activity. Urease is considered closely associated with the transformation of N, and its activity was positively correlated with the concentration of NO_3^- -N and had no significant correlation with metal(loid)s, which is similar to the results of Milosavljevic et al. (2020). The activity of β -glucosidase related to the C cycle had no significant relationship to soil properties and metal(loid). These results regarding enzyme activities manifest the complexity of the responses of soil enzyme activities to the environment (Milosavljevic et al., 2020).

Biological parameters like SBR, MBC, and qCO_2 are important indices for estimating soil pollution (Tang et al., 2022). SBR and MBC had significant negative correlations with P_N but no significant correlation with the single metal(loid) concentration, indicating that compound metal(loid) contamination might cause a reduction in SBR and MBC. Song et al. (2018) demonstrated that the synergistic effects of heavy metals on MBC were greater than those of single metals. Possible reasons for the reduction in microbial biomass may be that some microorganisms died under the stress of heavy metals or that the microorganisms transferred more energy to maintain the normal physiological function of cells, leading to a decrease in the amount of substrate utilized for the growth and reproduction of microorganisms (Tang et al., 2019; Zhang et al., 2016). However, it was found that microbial qCO_2 had no significant relationship with metal(loid) content, which conformed with the finding of Tang et al. (2022) that metal(loid) pollution had an inhibitory consequence on qCO_2 to some extent, but there was poor correlation between qCO_2 and metal(loid) content.

The correlation analysis indicated that the PAO rate was negatively correlated with total As. Some previous studies have pointed out that As can markedly inhibit soil nitrification (Subrahmanyam et al., 2014; Yu et al., 2021). There was a significant positive correlation between the PAO rate and the copy number of the *amoA* gene of AOB and AOA, manifesting the intrinsic connections between AOB, AOA with the PAO (Nahar et al., 2020; Subrahmanyam et al., 2014). These results further confirmed that AOB and AOA mediate soil nitrification. Furthermore, the PAO rate and abundance of AOB and AOA were negatively correlated with NH_4^+ -N and positively cor-

related with NO_3^- -N. Li et al. (2021a) also demonstrated that *amoA* gene abundance of AOB had a significant positive relationship with NO_3^- -N. The possible interpretation is that the higher PAO rates of soil promoted the transformation of NH_4^+ -N into NO_3^- -N, leading to higher consumption of NH_4^+ -N and a larger accumulation of NO_3^- -N in soil. Moreover, NH_4^+ -N and NO_3^- -N are the important factors in shaping the microbial community structure (Zou et al., 2021), which could be inferred that the change in N content may alter the microbial community structure and then change the soil N cycling process.

Considering the large number of microbial indicators and environmental variables, PCA was performed to reduce the dimension of original variables and to extract the principal variables. In our study, the extractable Sb and pH were found to be the main variables in the first dimension and the second dimension, respectively, which have the similarity to previous studies that extractable Sb and pH played a dominant role in affecting soil microorganisms in Xikuangshan mining area (Li et al., 2021b; Sun et al., 2022; Wang et al., 2022). These results further support the previous statement that the bioavailable concentrations of heavy metals and physicochemical properties promoted the shifts of microbial characteristics at disturbed sites (Batista et al., 2020). It is noteworthy that the relationship between microbial indicators and environmental factors established by correlation analysis and PCA has certain limitations in this study, which still need more evidence to verify their applicability in different types of contaminated soil.

3.4. Establishment of microbial indicators for soil pollution assessment

Soil microbial characteristics can reflect the ecological conditions and biological activity of contaminated soil and can be used as bioindicators to assess the pollution status of soils (Niemeyer et al., 2012). As mentioned above, FDA hydrolase activity had significant negative relationships to extractable Sb and P_N , indicating its sensitivity to Sb and comprehensive metal(loid) pollution in mining environment. FDA hydrolysis activity also showed susceptibility to Sb in the spiked experiment (Wang et al., 2021). Therefore, FDA hydrolysis activity could be considered as a potential biomarker to evaluate soil Sb and comprehensive metal(loid) contamination. Besides, it could be seen that acid phosphatase activity was negatively correlated with compound pollution degree of heavy metal, which demonstrated that acid phosphatase also could be used as a potential indicator to reflect changes in soil. Aponte et al. (2020a) pointed out that acid phosphatase, dehydrogenase and urease were sensitive to metal(loid) contamination. However, dehydrogenase and urease activities did not exhibit strong sensitivity to metal(loid) pollution in our study. Moreover, SBR and MBC might be proposed as good endpoints to define the impact of combined metal(loid)s on soil biological functioning due to their negative correlation with P_N .

According to the negative relationship between PAO rate and total As, it could be speculated that PAO rate could be utilized as an effective parameter to diagnose the As pollution in soil. However, the abundance of AOB and AOA was only associated with the N content in soil and had no significant asso-

ciation with metal(loid)s, which indicated that AOB and AOA abundance might not be the effective predictors in diagnosing soil metal(loid) contamination in Sb deposit. At present, using gene copy number of AOB and AOA to identify heavy metal contamination has not reached a consensus (Tang et al., 2019). It is noteworthy that the microbial indicators established in this study for metal(loid) pollution assessment still need more evidence to verify their applicability in different types of contaminated soil.

4. Conclusion

This research analyzed the metal(loid) pollution of soils in the Xikuangshan Sb deposit area and revealed the response relationship between microbial characteristics and metal(loid)s and soil physicochemical properties. The results indicated that the soils in the mining area were mainly polluted by Sb, As and Cd and that the pollution of Zn, Cu and Cr was not serious. The pollution degree of metal(loid)s differed among the sampling sites, in which the S1 sampling site had a slight pollution level, but other sampling sites reached severe contamination. Hierarchical cluster analysis showed that the mining soils polluted by metal(loid) pollution were highly discriminated by soil microbial parameters. Extractable Sb and pH played a dominant role in the soil environment of Xikuangshan mining area. The correlation analysis suggested that FDA hydrolase, acid phosphatase, SBR and MBC were negatively correlated with P_N , suggesting their sensitivity to comprehensive metal(loid) contamination. In addition, dehydrogenase, urease, PAO rate and abundance of AOB and AOA were susceptible to pH or N contents. These findings can provide fundamental information for soil ecological risk assessment and environmental management to protect soil ecosystems in Sb mining area. However, our study only discussed the response of soil microbial activity and ammonia oxidation to environmental factors in a specific mining environment and requires further validation in other soil types.

Declaration of Competing Interest

The authors declare that they have no known competing financial interests or personal relationships that could have appeared to influence the work reported in this paper.

Acknowledgment

This work was supported by the National Natural Science Foundation of China (No. 42030706).

Appendix A Supplementary data

Supplementary data associated with this article can be found in the online version at doi:10.1016/j.jes.2022.07.003.

REFERENCES

- Adam, G., Duncan, H., 2001. Development of a sensitive and rapid method for the measurement of total microbial activity using fluorescein diacetate (FDA) in a range of soils. *Soil Biol. Biochem.* 33, 943–951.
- Anderson, T.H., Domsch, K.H., 1993. The metabolic quotient for CO₂ (qCO₂) as a specific activity parameter to assess the effects of environmental conditions, such as pH, on the microbial biomass of forest soils. *Soil Biol. Biochem.* 25, 393–395.
- Aponte, H., Medina, J., Butler, B., Meier, S., Cornejo, P., Kuzyakov, Y., 2020a. Soil quality indices for metal(loid) contamination: An enzymatic perspective. *Land Degrad. Dev.* 31, 2700–2719.
- Aponte, H., Meli, P., Butler, B., Paolini, J., Matus, F., Merino, C., et al., 2020b. Meta-analysis of heavy metal effects on soil enzyme activities. *Sci. Total Environ.* 737, 139744.
- Aponte, H., Mondaca, P., Santander, C., Meier, S., Paolini, J., Butler, B., et al., 2021. Enzyme activities and microbial functional diversity in metal(loid) contaminated soils near to a copper smelter. *Sci. Total Environ.* 779, 146423.
- Bagherifarn, S., Brown, T.C., Fellows, C.M., Naidu, R., 2019. Derivation methods of soils, water and sediments toxicity guidelines: A brief review with a focus on antimony. *J. Geochem. Explor.* 205, 106348.
- Bahram, M., Hildebrand, F., Forslund, S.K., Anderson, J.L., Soudzilovskaia, N.A., Bodegom, P.M., et al., 2018. Structure and function of the global topsoil microbiome. *Nature* 560, 233–237.
- Batista, É.R., Carneiro, J.J., Araújo Pinto, F., dos Santos, J.V., Carneiro, M.A.C., 2020. Environmental drivers of shifts on microbial traits in sites disturbed by a large-scale tailing dam collapse. *Sci. Total Environ.* 738, 139453.
- Bolan, N., Kumar, M., Singh, E., Kumar, A., Singh, L., Kumar, S., et al., 2022. Antimony contamination and its risk management in complex environmental settings: A review. *Environ. Int.* 158, 106908.
- Cappuyns, V., Van Campen, A., Helsler, J., 2021. Antimony leaching from soils and mine waste from the Mau Due antimony mine, North-Vietnam. *J. Geochem. Explor.* 220, 106663.
- Cheng, J., Shi, Z., Zhu, Y.W., 2007. Assessment and mapping of environmental quality in agricultural soils of Zhejiang Province, China. *J. Environ. Sci.* 19, 50–54.
- Das, S., Jean, J.S., Kar, S., Chakraborty, S., 2013. Effect of arsenic contamination on bacterial and fungal biomass and enzyme activities in tropical arsenic-contaminated soils. *Biol. Fert. Soils* 49, 757–765.
- Dick, R.P., 2011. *Methods of Soil Enzymology*. Soil Science Society of America, Inc, Madison, Wisconsin, USA.
- Ettler, V., Mihaljevic, M., Sebek, O., Nechutny, Z., 2007. Antimony availability in highly polluted soils and sediments - A comparison of single extractions. *Chemosphere* 68, 455–463.
- Feyzi, H., Chorom, M., Bagheri, G., 2020. Urease activity and microbial biomass of carbon in hydrocarbon contaminated soils. A case study of cheshmeh-khosh oil field, Iran. *Ecotox. Environ. Safe.* 199, 110664.
- Filella, M., Belzile, N., Chen, Y.W., 2002. Antimony in the environment—a review focused on natural waters-I. Occurrence. *Earth-Sci. Rev.* 57, 125–176.
- Gong, W.J., Niu, Z.F., Wang, X.R., Zhao, H.P., 2021. How the soil microbial communities and activities respond to long-term heavy metal contamination in electroplating contaminated site. *Microorganisms* 9 (2), 362.
- Gruen, A.L., Straskraba, S., Schulz, S., Schloter, M., Emmerling, C., 2018. Long-term effects of environmentally relevant concentrations of silver nanoparticles on microbial biomass, enzyme activity, and functional genes involved in the nitrogen cycle of loamy soil. *J. Environ. Sci.* 69, 12–22.
- Guo, X.J., Wang, K.P., He, M.C., Liu, Z.W., Yang, H.L., Li, S.S., 2014. Antimony smelting process generating solid wastes and dust: Characterization and leaching behaviors. *J. Environ. Sci.* 26, 1549–1556.
- He, H., Liu, H., Shen, T., Wei, S., Dai, J., Wang, R., 2018. Influence of Cu application on ammonia oxidizers in fluvo-aquic soil. *Geoderma* 321, 141–150.
- He, M.C., Wang, N.N., Long, X.J., Zhang, C.J., Ma, C.L., Zhong, Q.Y., et al., 2019. Antimony speciation in the environment: Recent advances in understanding the biogeochemical processes and ecological effects. *J. Environ. Sci.* 75, 14–39.
- Insam, H., Hutchinson, T.C., Reber, H.H., 1996. Effects of heavy metal stress on the metabolic quotient of the soil microflora. *Soil Biol. Biochem.* 28, 691–694.
- Li, H., Yao, J., Min, N., Liu, J.L., Chen, Z.H., Zhu, X.Z., et al., 2022. Relationships between microbial activity, enzyme activities and metal(loid) form in NiCu tailings area. *Sci. Total Environ.* 812, 152326.
- Li, M., Zhang, J., Yang, X., Zhou, Y., Zhang, L., Yang, Y., et al., 2021a. Responses of ammonia-oxidizing microorganisms to biochar and compost amendments of heavy metals-polluted soil. *J. Environ. Sci.* 102, 263–272.
- Li, N., Chen, Y., Zhang, Z., Chang, S., Huang, D., Chen, S., et al., 2019. Response of ammonia-oxidizing archaea to heavy metal contamination in freshwater sediment. *J. Environ. Sci.* 77, 392–399.
- Li, Y., Zhang, M., Xu, R., Lin, H., Sun, X., Xu, F., et al., 2021b. Arsenic and antimony co-contamination influences on soil microbial community composition and functions: Relevance to arsenic resistance and carbon, nitrogen, and sulfur cycling. *Environ. Int.* 153, 106522.
- Liu, J., Yao, J., Lu, C., Li, H., Li, Z.F., Duran, R., et al., 2019. Microbial activity and biodiversity responding to contamination of metal(loid) in heterogeneous nonferrous mining and smelting areas. *Chemosphere* 226, 659–667.
- Liu, J., Cao, W., Jiang, H., Cui, J., Shi, C., Qiao, X., et al., 2018. Impact of heavy metal pollution on ammonia oxidizers in soils in the vicinity of a tailings dam, Baotou, China. *B. Environ. Contam. Tox.* 101, 110–116.
- Liu, K., Li, C., Tang, S., Shang, G., Yu, F., Li, Y., 2020. Heavy metal concentration, potential ecological risk assessment and enzyme activity in soils affected by a lead-zinc tailing spill in Guangxi, China. *Chemosphere* 251, 126415.
- Milosavljevic, J.S., Serbula, S.M., Cokesa, D.M., Milanovic, D.B., Radojevic, A.A., Kalinovic, T.S., et al., 2020. Soil enzyme activities under the impact of long-term pollution from mining-metallurgical copper production. *Eur. J. Soil Biol.* 101, 103232.
- Murciego Murciego, A., Garcia Sanchez, A., Rodriguez Gonzalez, M.A., Pinilla Gil, E., Toro Gordillo, C., Cabezas Fernandez, J., et al., 2007. Antimony distribution and mobility in topsoils and plants (*Cytisus striatus*, *Cistus ladanifer* and *Dittrichia viscosa*) from polluted Sb-mining areas in Extremadura (Spain). *Environ. Pollut.* 145, 15–21.
- Nahar, K., Ali, M.M., Khanom, A., Alama, M.K., Azad, M.A.K., Rahman, M.M., 2020. Levels of heavy metal concentrations and their effect on net nitrification rates and nitrifying archaea/bacteria in paddy soils of Bangladesh. *Appl. Soil Ecol.* 156, 103697.
- Nguyen, T.H., Won, S., Ha, M.G., Nguyen, D.D., Kang, H.Y., 2021. Bioremediation for environmental remediation of toxic metals and metalloids: A review on soils, sediments, and mine tailings. *Chemosphere* 282, 131108.
- Niemeyer, J.C., Lolata, G.B., de Carvalho, G.M., Da Silva, E.M., Sousa, J.P., Nogueira, M.A., 2012. Microbial indicators of soil

- health as tools for ecological risk assessment of a metal contaminated site in Brazil. *Appl. Soil Ecol.* 59, 96–105.
- Okkenhaug, G., Zhu, Y.G., Luo, L., Lei, M., Li, X., Mulder, J., 2011. Distribution, speciation and availability of antimony (Sb) in soils and terrestrial plants from an active Sb mining area. *Environ. Pollut.* 159, 2427–2434.
- Pedro Martin-Sanz, J., Valverde-Asenjo, I., de Santiago-Martin, A., Ramon Quintana-Nieto, J., Gonzalez-Huecas, C., Lopez-Lafuente, A.L., et al., 2018. Enzyme activity indicates soil functionality affectation with low levels of trace elements. *Environ. Pollut.* 243, 1861–1866.
- Qin, Z., Zhao, S., Shi, T., Zhang, F., Pei, Z., Wang, Y., Liang, Y., 2022. Accumulation, regional distribution, and environmental effects of Sb in the largest Hg–Sb mine area in Qinling Orogen, China. *Sci. Total. Environ.* 804, 150218.
- Raiesi, F., Sadeghi, E., 2019. Interactive effect of salinity and cadmium toxicity on soil microbial properties and enzyme activities. *Ecotox. Environ. Safe.* 168, 221–229.
- Song, J., Shen, Q., Wang, L., Qiu, G., Shi, J., Xu, J., et al., 2018. Effects of Cd, Cu, Zn and their combined action on microbial biomass and bacterial community structure. *Environ. Pollut.* 243, 510–518.
- Subrahmanyam, G., Hu, H.W., Zheng, Y.M., Archana, G., He, J.Z., Liu, Y.R., 2014. Response of ammonia oxidizing microbes to the stresses of arsenic and copper in two acidic alfisols. *Appl. Soil Ecol.* 77, 59–67.
- Sun, W., Xiao, E., Xiao, T., Krumins, V., Wang, Q., Haggblom, M., et al., 2017. Response of soil microbial communities to elevated antimony and arsenic contamination indicates the relationship between the innate microbiota and contaminant fractions. *Environ. Sci. Technol.* 51, 9165–9175.
- Sun, X., Kong, T., Li, F., Haggblom, M.M., Kolton, M., Lan, L., et al., 2022. *Desulfurivibrio* spp. mediate sulfur-oxidation coupled to Sb(V) reduction, a novel biogeochemical process. *ISME J.* 16, 1547–1556.
- Tang, B., Xu, H., Song, F., Ge, H., Yue, S., 2022. Effects of heavy metals on microorganisms and enzymes in soils of lead-zinc tailing ponds. *Environ. Res.* 207, 112174.
- Tang, J., Zhang, J., Ren, L., Zhou, Y., Gao, J., Luo, L., et al., 2019. Diagnosis of soil contamination using microbiological indices: A review on heavy metal pollution. *J. Environ. Manage.* 242, 121–130.
- USEPA (U.S. Environmental Protection Agency), 2005. Ecological Soil Screening Levels for Antimony: Interim Final. Office of Solid Waste and Emergency Response, Washington, DC OSWER Directive 9285.7-61. Available:.
- USGS (U.S. Geological Survey), 2022. Mineral Commodity Summaries 2022 - Antimony. U.S. Geological Survey Available: Accessed January 31, 2022 doi:10.3133/mcs2022.
- Vance, E.D., BrggkeR, P.C., Jenkin, D.S., 1987. An extraction method for measuring soil microbial biomass C. *Soil Biol. Biochem.* 19 (6), 657–786.
- Wang, A.H., He, M.C., Ouyang, W., Lin, C.Y., Liu, X.T., 2021. Effects of antimony (III/V) on microbial activities and bacterial community structure in soil. *Sci. Total. Environ.* 789, 148073.
- Wang, N.N., Wang, A.H., Xie, J., He, M.C., 2019. Responses of soil fungal and archaeal communities to environmental factors in an ongoing antimony mine area. *Sci. Total. Environ.* 652, 1030–1039.
- Wang, W., Wang, H., Cheng, X., Wu, M., Song, Y., Liu, X., et al., 2022. Different responses of bacteria and fungi to environmental variables and corresponding community assembly in Sb-contaminated soil. *Environ. Pollut.* 298, 118812.
- Wang, Y.P., Shi, J.Y., Lin, Q., Chen, X.C., Chen, Y.X., 2007. Heavy metal availability and impact on activity of soil microorganisms along a Cu/Zn contamination gradient. *J. Environ. Sci.* 19, 848–853.
- Wang, Y., Zeng, X., Zhang, Y., Zhang, N., Xu, L., Wu, C., 2023. Responses of potential ammonia oxidation and ammonia oxidizers community to arsenic stress in seven types of soil. *J. Environ. Sci.* 127, 15–29.
- Wei, Y., Chen, Z., Wu, F., Hou, H., Li, J., Shangguan, Y., et al., 2015. Molecular diversity of arbuscular mycorrhizal fungi at a large-scale antimony mining area in southern China. *J. Environ. Sci.* 29, 18–26.
- Yang, J., Yang, F., Yang, Y., Xing, G., Deng, C., Shen, Y., et al., 2016. A proposal of "core enzyme" bioindicator in long-term Pb-Zn ore pollution areas based on topsoil property analysis. *Environ. Pollut.* 213, 760–769.
- Yu, H., Zheng, X., Weng, W., Yan, X., Chen, P., Liu, X., et al., 2021. Synergistic effects of antimony and arsenic contaminations on bacterial, archaeal and fungal communities in the rhizosphere of *Miscanthus sinensis*: Insights for nitrification and carbon mineralization. *J. Hazard. Mater.* 411, 125094.
- Zhang, C., Nie, S., Liang, J., Zeng, G., Wu, H., Hua, S., et al., 2016. Effects of heavy metals and soil physicochemical properties on wetland soil microbial biomass and bacterial community structure. *Sci. Total. Environ.* 557, 785–790.
- Zhang, F., Li, C., Tong, L., Yue, L., Li, P., Ciren, Y., et al., 2010. Response of microbial characteristics to heavy metal pollution of mining soils in central Tibet, China. *Appl. Soil Ecol.* 45, 144–151.
- Zhang, S.H., Wang, Y., Pervaiz, A., Kong, L.H., He, M.C., 2018. Comparison of diffusive gradients in thin-films (DGT) and chemical extraction methods for predicting bioavailability of antimony and arsenic to maize. *Geoderma* 332, 1–9.
- Zhou, Z.F., Liu, Y.R., Sun, G.X., Zheng, Y.M., 2015. Responses of soil ammonia oxidizers to a short-term severe mercury stress. *J. Environ. Sci.* 38, 8–13.
- Zhu, X., Yao, J., Wang, F., Yuan, Z., Liu, J., Jordan, G., et al., 2018. Combined effects of antimony and sodium diethyldithiocarbamate on soil microbial activity and speciation change of heavy metals. Implications for contaminated lands hazardous material pollution in nonferrous metal mining areas. *J. Hazard. Mater.* 349, 160–167.
- Zou, L., Lu, Y., Dai, Y., Khan, M.I., Gustave, W., Nie, J., et al., 2021. Spatial variation in microbial community in response to As and Pb contamination in paddy soils near a Pb-Zn mining site. *Front. Environ. Sci.* 9, 630668.